Self-Assembly of a Molecular Capsule Driven by Electrostatic Interaction in Aqueous Solution

Bertrand Hamelin,[†] Ludovic Jullien,*[,†] Christiane Derouet,[†] Catherine Hervé du Penhoat,*[,†] and Patrick Berthault[‡]

Contribution from the Département de Chimie (CNRS URA 1679), Ecole Normale Supérieure, 24 rue Lhomond, F-75231 Paris Cedex 05, France, and DRECAM/SCM, CEA, CE Saclay, F-91191 Gif s/s Yvette Cedex, France

Received January 5, 1998

Abstract: A self-assembling molecular capsule based on electrostatic interaction has been designed and its structure is investigated by dynamic ^{1}H NMR. The hydrodynamic description resulting from relaxation and PGSE ^{1}H NMR experiments indicates that association between oppositely charged hydrophilic β-cyclodextrin derivatives in 50 mM KCl aqueous solution corresponds to dimerization with an interdistance between interacting units lying in the 0.4−1.1 nm range with a maximal probability at 0.6 nm.

Introduction

The control of intermolecular interactions in condensed phase represents a goal for many chemists. These issues have been addressed either experimentally or theoretically on a variety of systems involving different scales or ranges and different types of intermolecular forces; many concepts are now available to predict interaction behaviors at nanoscopic or macroscopic scales.[1,2] In supramolecular chemistry, these concepts have been used to build large self-assembled artificial systems[3] in solution such as helicates,[4] rosettes,[5] molecular capsules,[6] ... . Such arrays result from the spontaneous organization of large molecular units of similar size that interact according to a predefined scheme. Up to now, most efforts have been devoted to the use of short-range attractive interactions (hydrogen bonding, coordination, ...) in organic solvents.

Considering that electrostatic interaction between charged bodies often has been successfully rationalized (solid ionic lattices of low valency ions,[7] colloidal crystals,[8] host−guest[9] or biological[10] complexes, ...), we have decided to investigate the potential of the long-range charge−charge interaction for building large self-assembled systems in aqueous solution. In the present paper, we present a new type of molecular capsule resulting from the self-association between oppositely charged hollow bodies in aqueous solution. Several features of the system offer new perspectives for the control of substrate encapsulation within self-assembled capsules: the charge-induced polarization to modify the electronic properties of the substrate, the possibility to tune the complex stability or the overall charges of the whole assembly, ...

The β-cyclodextrin backbone has been chosen as the elementary unit to build a molecular capsule based on electrostatic interaction.[11] The rational for molecular design stems from energetic considerations involving the following: (i) prevention of the interacting units from reorganizing their backbone to minimize their energy through intramolecular deformations decreasing the electrostatic repulsion between identically charged groups; (ii) prevision for complementarity between oppositely highly charged species by means of planar surfaces bearing identical charge distribution; (iii) elimination of the formation of large aggregates by screening undesirable electrostatic interactions by using the cyclodextrin backbone as a spacer; and (iv) avoiding the precipitation of associated species by working with hydrophilic interacting species independently of the presence of charges.

In a previous report,[12] it was shown that per-6-amino β-cyclodextrin CD7(Am) and per-6-thioglycolic β-cyclodextrin CD7(Ac) strongly interact at neutral pH (Figure 1). In the present paper, the stoichiometry and the structure of the CD7(Am):CD7(Ac) associated species are now reported. Besides its relevance for building a new type of molecular capsule, this

* To whom correspondence should be addressed at Département de Chimie (URA 1679). Telefax number: 00 33 (0)1 44 32 33 25. E-mail address: Ludovic.Jullien@ens.fr.

[†] Ecole Normale Supérieure.

[‡] DRECAM/SCM.

(1) Israelachivili, J. *Intermolecular and Surface Forces*, 2nd ed.; Academic Press: New York, 1991.

(2) Gerschel, A. *Liaisons intermoléculaires*; InterEditions et CNRS Editions: Paris, 1995.

(3) *Comprehensive Supramolecular Chemistry*; Lehn, J.-M., Atwood, J. L., Davies, J. E. D., MacNicol, D. D., Vögtle, F., Eds.; Pergamon: New York, 1996.

(4) For a review, see: Piguet, C.; Bernardinelli, G.; Hopfgartner. *Chem. Rev*. **1997**, *97*, 2005−2062.

(5) For a review on this topic, see: Whitesides, G. M.; Simanek, E. E.; Mathias, J. P.; Seto, C. T.; Chin, D. N.; Mammen, M.; Gordon, D. M. *Acc. Chem. Res.* **1995**, *28*, 37−44.

(6) For a review, see: Conn, M. M.; Rebek, J. *Chem. Rev.* **1997**, *97*, 1647−1668.

(7) Huheey, J. E. *Inorganic Chemistry: Principles of Structure and Reactivity*, 3rd ed.; Harper and Row: New York, 1983.

(8) Forsyth, P. A.; Marcelja, S.; Mitchell, D. J.; Ninham, B. W. *Adv. Colloid Interface Sci.* **1978**, *9*, 37−60.

(9) For reviews see: Schneider, H.-J. *Angew. Chem., Int. Ed. Engl.* **1991**, *30*, 1417−1436. Schneider, H.-J. *Chem. Soc. Rev*. **1994**, *23*, 227−234 and references therein.

(10) Davis, M. E.; McCammon, J. A. *Chem. Rev.* **1990**, *90*, 509−521. Sharp, K. A. *Curr. Op. Struct. Biol*. **1994**, *4*, 234−239. Gilson, M. K. *Curr. Op. Struct. Biol*. **1995**, *5*, 216−223. Sharp, K. A.; Honig, B. *Curr. Op. Struct. Biol*. **1995**, *5*, 323−328. Misra, V. K.; Sharp, K. A.; Friedman, R. A.; Honig, B. *J. Mol. Biol.* **1994**, *238*, 245−263. Misra, V.; Hecht, J. L.; Sharp, K. A.; Friedman, R. A.; Honig, B. *J. Mol. Biol.* **1994**, *238*, 264−280.

(11) Guillo, F.; Jullien, L.; Hamelin, B.; Lehn, J.-M.; De Robertis, L.; Driguez, H. *Bull. Soc. Chim. Fr*. **1995**, *132*, 857−866.

(12) Hamelin, B.; Jullien, L.; Guillo, F.; Lehn, J.-M.; Jardy, A.; De Robertis, L.; Driguez, H. *J. Phys. Chem.* **1995**, *99*, 17877−17885.

S0002-7863(98)00046-8 CCC: $15.00
Published on Web 08/07/1998

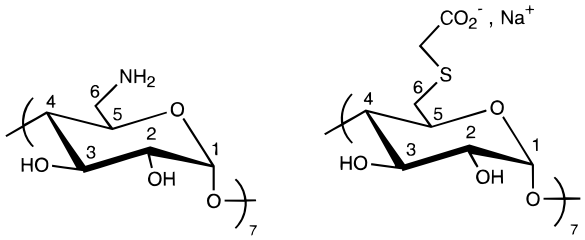

Figure 1. Chemical structure of CD7(Am) (left) and CD7(Ac) (right).

investigation additionally (i) evaluates dynamic NMR experiments for deducing hydrodynamic and structural properties of large self-assembled supramolecular assemblies and (ii) addresses the issue of the average distance at equilibrium between oppositely charged bodies in aqueous solution.

Results

In the millimolar concentration range, NMR is a powerful tool to elucidate structures in solution.[13] A complete NMR investigation may shed light not only on average atomic coordinates over accessible conformations, but also on molecular dynamics. In the present study, chemical shifts and coupling constants of the β-cyclodextrin derivatives CD7(Am) and CD7(Ac), either alone or mixed, were examined in a first step to evidence any major structural change occurring upon association. Then dynamic NMR has been used to measure the translational diffusion coefficients and correlation times of CD7(Am) or CD7(Ac) (i) alone, in relation to the molecular structure and (ii) in the CD7(Am):CD7(Ac) mixture, to eventually extract the structure of the CD7(Am):CD7(Ac) associated species. In view of the limited solubility of the different species (see Experimental Section), we concentrated on the use of ^{1}H NMR in the present study.

^{1}H NMR. Chemical Shift Assignment and Coupling Constant Data. 1D 400 MHz ^{1}H NMR spectra of the 2 mM solutions of CD7(Ac), CD7(Am), or the 1 mM CD7(Ac):CD7(Am) 1:1 mixture were recorded in 50 mM KCl in D_2O at pH = 6.2 (see experimental part). From the previous investigation,[12] it was shown that the CD7(Ac):CD7(Am) 1:1 mixture contained only associated species at concentrations as low as 1 mM.[14] The fine structure of the ^{1}H NMR spectrum of the CD7(Ac):CD7(Am) associated species was identical to that of the individual compounds with the exception of the methylene group belonging to the thioacetic group of CD7(Ac). From a quasi A_2 system (broad singlet) in pure CD7(Ac), it evolved in the mixture to an AB system (chemical shift separation of 25 Hz, J_{AB} value of 13.4 Hz). Moreover small (<0.15 ppm) upfield (H5(Am); H4,H6b(Ac)) or downfield (H6a(Am); $-CH_2-S-$, H6a(Ac)) shifts were observed for most of the other signals when compared to those of the individual components at the same pH (Table 1). With the hope to get some information related to the change of protonation state or environment linked to any CD7(Ac):CD7(Am) interaction, these shifts have been related to the shifts of the ^{1}H chemical shifts of individual compounds that are induced by pH changes. Figures 2a and 2b respectively display the chemical shifts of the CD7(Am) and CD7(Ac) protons as a function of pH (2 mM solutions of CD7(Am) and CD7(Ac) in 50 mM KCl in D_2O).[15] In the range of investigated pH, the CD7(Ac) protons are essentially unaffected by pH modifications whereas the H6(Am) are the most sensitive signals in CD7(Am). These observations are in line with (i) the respective pK_a of the CD7(Ac) and the CD7(Am) units[12] that determine the pH range over which the protonation states of CD7(Ac) ($2 < pH < 7$) and CD7(Am) ($6 < pH < 11$) should evolve; (ii) the closest proximity of the observed protons to the ionizable groups in CD7(Am) rather than in CD7(Ac) that induces larger shifts in the former case; (iii) the larger electron-withdrawing ability of the ammonium group with regards to the amino group ($\Delta\delta < 0$ for $\Delta pH > 0$); and (iv) the closest proximity of the H6 position to the ionizable group in CD7(Am). From the preceding chemical shift calibration as a function of pH, it should be easy to extract the protonation states of CD7(Ac) and CD7(Am) either as individual compounds or as associated species at any pH. In fact, at a given pH, the difference in protonation states between individual and associated species is linked to the interaction potential and thus to the Gibbs free energy of association.[16] Nevertheless, in view of the weakness of the effect of pH on CD7(Ac) and CD7(Am) chemical shifts (at the most $\Delta\delta \approx -0.2$ ppm for $\Delta pH = +4$ for H6(Am)) and due to the possible interferences that should be caused by the change of proton environment upon association, chemical shifts were not used for investigating CD7(Ac):CD7(Am) association.

In all investigated systems, the vicinal proton coupling constants ^3J between cyclodextrin methine protons indicated the classical $^4C_1$ conformer for the sugar rings. Furthermore, rotamer populations of CD7(Am) and CD7(Ac), alone or associated, have been extracted from the $^3J^{\,exp}_{5,6a}$ and $^3J^{\,exp}_{5,6b}$ vicinal coupling constants (Table 2; see Experimental Section). Upon considering only the three staggered conformers GG, GT, and TG, simulations pointed to a 1:1 (respectively 1:2) GG:GT average for CD7(Ac) (respectively for CD7(Am)) for the isolated species and a 1:2 (respectively 1:3) GG:GT average for CD7(Ac) (respectively for CD7(Am)) for the CD7(Am):CD7(Ac) associated species. Thus, the coupling constant analysis suggested that although no major conformational change in the cyclodextrin backbone had taken place upon association, a significant modification in the average pendant arm orientation had occurred upon association.

Quantitative ^{1}H-NOESY Spectra. For a multi-spin system, the integrated intensity of a cross-peak between two protons *i*

(13) Cantor, C. R.; Schimmel, P. R. *Biophysical Chemistry*, Part II; Freeman: New York, 1980.

(14) In the previous paper,[12] equilibrium constants *K* have been estimated to log $K \approx 10$ at pH ≈ 6 and monovalent salt concentrations around 10−20 mM. Careful investigations on comparable biological systems have demonstrated the equilibrium constants for such electrostatically induced associations not to drop by more than 2 orders of magnitude when going from 10−20 mM to 50 mM (see: Mascotti, D. P.; Lohman, T. M. *Proc. Natl. Acad. Sci. U.S.A.* **1990**, *87*, 3142−3146). On such a basis, one thus expects the exclusive formation of the CD7(Ac):CD7(Am) associated species under the present experimental conditions (CD7(Ac):CD7(Am) 1:1 mixture 1 mM in KCl 50 mM at pH = 6.2).

(15) These NMR data have been used to check the CD7(Am) acidobasic constants that were determined by potentiometry in the previous investigation.[12] Under the observed regime of fast exchange for the ionizable protons of CD7(Am) at a given pH, the average chemical shift of any proton i is expressed by $\bar{\delta}_i(pH) = p_{NH_3^+}(pH)\delta_i(NH_3^+) + p_{NH_2}(pH)\delta_i(NH_2)$, where $p_x(pH)$ and $\delta_i(x)$ respectively designate the proportions of the x group in CD7(Am) at a given pH and the asymptotic limit of the considered chemical shift δ_i when all the CD7(Am) groups are under the x form. If $p_\nu(pH)$ is the proportion of the $[CD7(Am)H_\nu]^{\nu+}$ species, one has: $p_{NH_3^+}(pH) = {}^1/_7\sum_{\nu=0}^{7}(\nu p_\nu(pH)$ and $p_{NH_2}(pH) = {}^1/_7\sum_{\nu=0}^{7}(7-\nu)p_\nu(pH)$. The $p_\nu(pH)$ and $p_x(pH)$ functions have been calculated from the pK_a of CD7(Am).[12] These functions then have been used to simulate the $\bar{\delta}_i(pH)$ functions for H1 and H6a. The Figure A, parts a and b, available as Supporting Information, displays the comparison between the experimental data and the simulated ones that have been obtained with the following values of $\delta_i(x)$: $\delta_{H1}(NH_3^+) = 5.191$ and $\delta_{H6\alpha}(NH_3^+) = 3.520$ (experimental values at low pH where all sites are protonated); and $\delta_{H1}(NH_2) = 5.105$ and $\delta_{H6\alpha}(NH_2) = 3.268$ that emerge from the fitting procedure. As shown on Figure A, the agreement between experimental and simulated data is satisfactory and confirms the pK_a values that were determined by potentiometry.

(16) Jullien, L.; Cottet, H.; Hamelin, B.; Jardy, A. Manuscript in preparation.

Table 1. ^{1}H-NMR Chemical Shifts of 2 mM CD7(Am), 2 mM CD7(Ac), and 1 mM CD7(Ac):CD7(Am) in 50 mM KCl in D_2O at pH 6.2 and 294 K (for numbering, see Figure 1)[a]

species	1	2	3	4	5	6a	6b	SCH_2
CD7(Am)	5.17	3.68	4.00	3.59	4.2	3.46	3.27	
	(d; 3.5)	(dd; 3.5, 10.5)	(dd; 9.5, 9.5)	(dd; 9.5, 9.5)	(m)	(dd; 3, 13)	(dd; 7.5, 13)	
CD7(Ac)	5.13	3.65	3.94	3.69	4.0	3.19	2.98	3.40
	(d; 3.5)	(dd; 3.5, 10.5)	(dd; 9.5, 9.5)	(dd; 9.5, 9.5)	(m)	(dd; 3, 14)	(dd; 6, 14)	(A_2)
CD7(Am):CD7(Ac)	5.16	3.70	4.00	3.58	4.15	3.48	3.25	
	(d; 3.5)	(dd; 3.5, 10)	(dd; 9.5, 9.5)	(dd; 9.5, 9.5)	(m)	(dd; 3, 13)	(dd; 8.2, 13)	
	5.10	3.65	3.90	3.60	4.0	3.24	2.90	3.45 and 3.38
	(d; 3.5)	(dd; 3.5, 1.0)	(dd; 9.5, 9.5)	(dd; 9.5, 9.5)	(m)	(dd; 3, 14)	(dd; 7.5, 14)	(AB, 14.5)

[a] The multiplicities and ^3J coupling constants are given in parentheses.

and j in a ^{1}H-NOESY spectrum is described as follows:

$$V_{\tau_m} = V_0 e^{-\Gamma\tau_m} \quad (1)$$

where V_0 and V_{τ_m} are the matrices of the NOESY volumes for mixing times of 0 and τ_m, respectively, and Γ is the relaxation matrix. In proton relaxation of sugars, the dipole−dipole mechanism dominates relaxation.[17] The terms of the relaxation matrix Γ, the relaxation constants R_{ij}, depend on the values of the dipolar spectral density functions at frequencies 0, ω, and 2ω (ω being the Larmor frequency), which describe the motion of each proton pair. To separate the structural contribution (generally the internuclear distance $\{r_{ij}\}$) from the purely dynamic part, a motion model has to be assumed. In organic chemistry, the principle of most structural determinations from quantitative NOESY spectra lies in extracting average distances from the relaxation matrix Γ by assuming a given tumbling motion of the molecule in solution.[18] Alternatively, if a molecular geometry $\{r_{ij}\}$ is known from crystallography or molecular modeling, it becomes possible to access the molecular motional behavior. Once $\{r_{ij}\}$ and $J(\omega)$ are defined, it is possible to calculate the NOESY spectra for different values of the correlation times and to compare them with the experimental NOESY spectrum. The best values of correlation times are then used to derive rotational diffusion coefficients that are finally transformed into molecular dimensions under the assumption of a given shape.[13]

Quantitative NOESY spectra were recorded at 294 K for two mixing times τ_m: 0 and 400 ms. The normalization procedure was performed as already reported.[19,20] The normalized NOESY volumes of the methine and the methylene protons for CD7-(Ac), CD7(Am), or CD7(Ac):CD7(Am) associated species for τ_m = 400 ms are given in Table 3 (see Experimental Section). The intramolecular cross-peaks of the associated species were much stronger than those of the individual species. The latter tendancy indicated that the molecular tumbling time of the complex was much longer than that of the individual species. As the overall tumbling time is a function of the molecular friction, this increase corroborated the association between oppositely charged species. Additionally, in the CD7(Ac):CD7-(Am) associated species, no *intermolecular* cross-peak could be unambiguously detected between the protons of CD7(Ac) and CD7(Am). Since the normalized *intramolecular* cross-peaks corresponding to fairly long intraresidue interproton distances such as those for H1/H3 (0.38 nm) were very weak (0.033), this observation suggested that the distance between interacting CD7(Ac) and CD7(Am) exceeded 0.4 nm.

Table 2. Experimental Coupling Constants and Corresponding GG, GT, and TG Rotamer Populations of CD7(Ac) and CD7(Am) in 2 mM CD7(Ac), 2 mM CD7(Am), and 1 mM CD7(Ac):CD7(Am) D_2O solutions with 50 mM KCl at pH 6.2 and 294 K (See Text and Experimental)

species	$^3J^{exp}_{5,6a}$ (Hz)	$^3J^{exp}_{5,6b}$ (Hz)	P_{GG}	P_{TG}	P_{GT}
CD7(Am)[a]	3	7.5	0.34	0.00	0.66
CD7(Ac)[b]	3	6	0.49	0.00	0.51
CD7(Am)[c]	3	8.2	0.27	0.00	0.73
CD7(Ac)[c]	3	7.5	0.34	0.00	0.66

[a] In CD7(Am) solution. [b] In CD7(Ac) solutions. [c] In CD7(Am):CD7(Ac) solution.

Table 3. Experimental 400.13 MHz ^{1}H Normalized NOESY Volumes of 2 mM Solutions of CD7(Ac), CD7(Am), and 1 mM CD7(Ac):CD7(Am) 1:1 Mixture in 50 mM KCl in D_2O at pH 6.2 and 294 K (Above, CD7(Am); middle, CD7(Ac); below, CD7(Ac):CD7(Am) 1:1 Mixture. See Text and Experimental Section)

	S1[a]	S2[b]	S3[c]	S4[d]	S5[e]	S6[f]	S7[g]
S1[a]	0.466			0.030			
	0.526			0.044			
	0.369		0.033	0.085			
S2[b]		0.560	0.033				
		0.611	0.126	0.034	0.045	0.032	
S3[c]			0.889				
			0.708				
			0.426				
S4[d]				0.730			
				0.722			
				0.626			
S5[e]					0.329	0.040	
					0.245		
					0.344	0.103	
S6[f]						0.354	
						0.120	0.044
						0.244	0.101
S7[g]							0.171
							0.241

[a] S1 = [H1(Ac) + H1(Am)]. [b] S2 = [H5(Am)]. [c] S3 = [H3(Ac) + H3(Am) + H5(Ac)]. [d] S4 = [H2(Ac) + H2(Am) + H4(Ac) + H4(Am)]. [e] S5 = [H6a(Am) + $SC\underline{H}_2$(a and b)(Ac)]. [f] S6 = [H6a(Ac) + H6b(Am)]. [g] S7 = [H6b(Ac)].

^{1}H NMR Translational Self-Diffusion Measurements. To corroborate the ^{1}H NMR relaxation data, we considered another suitable method that could independently be used to provide a hydrodynamic description of the CD7(Ac):CD7(Am) associated species in solution. The cyclodextrin translational self-diffusion coefficients D_t were measured in 50 mM KCl in D_2O at pH = 6.2 by ^{1}H NMR pulse gradients spin−echo (PGSE) experiments.[21] The D_t values determined at 294 K for the CD7(Ac), CD7(Am), or CD7(Ac):CD7(Am) associated species were 2.1,

(17) Poppe, L.; Van Halbeek, H. *Magn. Reson. Chem.* **1993**, *31*, 665−668.

(18) In general, the molecule is considered as a rigid body isotropically tumbling.

(19) Breg, J.; Kroon-Batenburg, L. M. J.; Strecker, G.; Montreuil, J.; Vliegenthart, J. F. G. *Eur. J. Biochem.* **1989**, *178*, 727−739.

(20) In the case of overlapping resonances, an average value was used for the normalization constant (see Experimental Section).

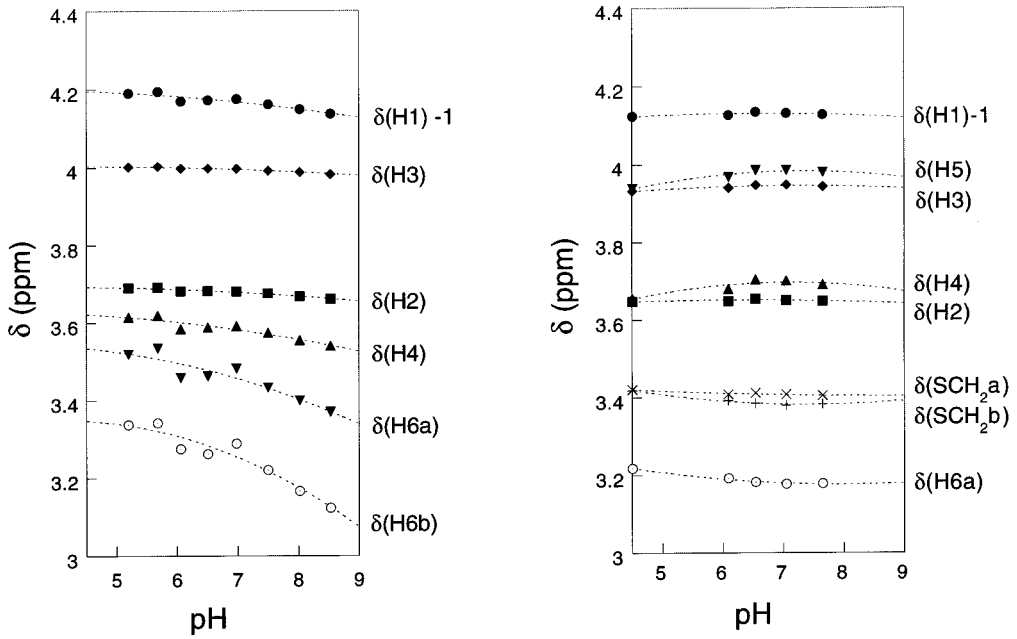

Figure 2. Calibration of chemical shifts in ^{1}H NMR for CD7(Am) (a: left) and CD7(Ac) (b: right). 2 mM solutions of CD7(Am) and CD7(Ac) in 50 mM KCl in D_2O. The chemical shifts of H5[CD7(Am)] and H6b[CD7(Ac)] are respectively obscured by H3[CD7(Am)] and by DSS so as to exclude their use. Internal reference: DSS (see experimental and text).

2.1, and $(1.5 \pm 0.1) \times 10^{-10}$ m^2 s^{-1}) (see Experimental Section). These results confirmed the observations that have been made from the NOESY data. As D_t is a decreasing function of molecular size, the notable drop in translational motion pointed out the interaction between the CD7(Ac) and CD7(Am) units in the CD7(Am):CD7(Ac) mixture.

Discussion

Since no intermolecular CD7(Am)−CD7(Ac) ^{1}H-NOESY cross-peaks within the CD7(Am):CD7(Ac) complex was observed, the relative atomic positions of the associated species could not be determined. Therefore, ^{1}H NMR data were used to provide a molecular description at a lower level of resolution. In agreement with their structural features, cyclodextrin interacting units have been treated as rigid[22] bodies of simple shape whose large size with regards to the diameter of the water molecule was compatible with considering the solvent as a continuum. The hydrodynamic behavior of associated species was then described in terms of shape and volume to deducing supramolecular organization (number and arrangement of constituting units) from the relations linking the rotational and translational diffusion coefficients to both the geometry and dimensions of rigid bodies of various shape.[23] In a first step, we sought a suitable description of the individual CD7(Am) and CD7(Ac) units in terms of hydrodynamics. Then, we attempted to derive a crude evaluation of the stoichiometry of the CD7(Am):CD7(Ac) associated species using a simple modelization of shape. Several physically plausible models of arrangements of interacting units finally have been considered to account for hydrodynamic properties of the CD7(Am):CD7-(Ac) complex and the best fit has been chosen to derive the structural information. Such an approach for structure determination has been successfully used in biochemistry, especially to solve nucleic acid[24] and quaternary proteic structures in solution.[25]

Description of CD7(Am) and CD7(Ac) Monomeric Units. From examination of Quanta molecular models, both CD7(Am) and CD7(Ac) monomeric units appear as truncated cones with an L/D aspect ratio (height/diameter = L/D) close to one. As a consequence, the overall motion exhibited by both molecules is expected to be isotropic and thus to be characterized by a single correlation time τ_c. For data analysis, we focused on the protons H1 to H5 borne by the cyclodextrin backbone since they were suggested to be the ones less prone to structural variations upon association from the examination of chemical shifts and coupling constants (Table 1). The Cartesian coordinates reported for the native β-cyclodextrin have been used to derive the $\{r_{ij}\}$ set since both the CD7(Am) and CD7(Ac) carbohydrate backbones can be considered structurally close to their native parent (see Experimental Section).[26] ^{1}H-NOESY simulations were performed for CD7(Am) for a considerable range of τ_c values (0.45−1.8 ns) that were expected to cover the reasonable range of hydrodynamic diameters for the β-cyclodextrin derived species ($1.5 < D$ (nm) < 2.5). The mean standard deviation R (see Experimental Section for definition) between experimental and simulated data was minimum for $\tau_c = 0.75 \pm 0.1$ ns (Figure 3). By assuming that stick boundary conditions[13] applied in view of the strong hydrophilic character

(21) Stilbs, P. *Prog. Nucl. Magn. Reson. Spectrosc.* **1984**, *19*, 1−45.

(22) When no functionalization is introduced on the secondary face, β-cyclodextrin backbones have been demonstrated to be rather rigid due to the stabilizing circular network of hydrogen bonds. See: Lipkowitz, K. B.; Green, K.; Yang, J. *Chirality* **1992**, *4*, 205−215. Lipkowitz, K. B. *J. Org. Chem.* **1991**, *56*, 6357−6367. Moreover, in the course of the different simulations presented in this paper, we examined the consequences of local internal motions on simulated data on several occasions by using the model-free approach described by Lipari and Szabo (Lipari, G.; Szabo, A. *J. Am. Chem. Soc.* **1982**, *104*, 4546−4559). We never observed any improvement that should have justified the systematic introduction of internal motions for NOESY simulations. The latter simulations have been used to evaluate error bars.

(23) Lamb, H. *Hydrodynamics*; Dover: New York, 1945.

(24) Eimer, W.; Williamson, J. R.; Boxer, S. G.; Pecora, R. *Biochemistry* **1990**, *29*, 799−811.

(25) Barbato, G.; Ikura, M.; Kay, L. E.; Pastor, R. W.; Bax, A. *Biochemistry* **1992**, *31*, 5269−5278.

(26) No attempt was made to model the charged species as relevant simulations would require the presence of numerous explicit solvent molecules and counterions which implied very long CPU times. See for instance: Young, M. A.; Jayaram, B.; Beveridge, D. L. *J. Am. Chem. Soc.* **1997**, *119*, 59−69.

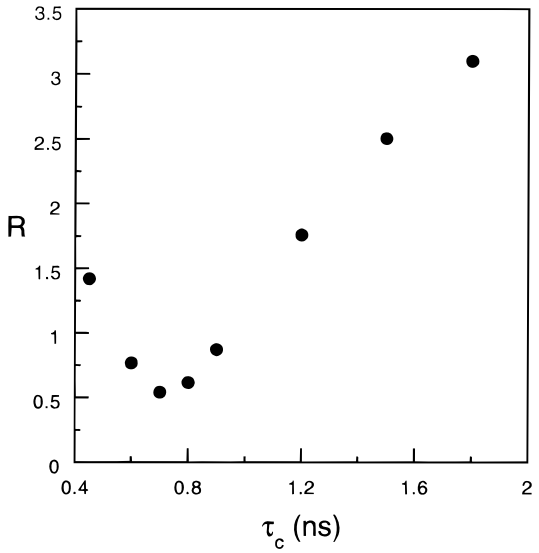

Figure 3. Mean standard deviation *R* between experimental and simulated quantitative NOESY spectra normalized volumes of CD7-(Am) as a function of the correlation time by assuming molecular isotropic tumbling (see the Experimental Section).

of both CD7(Am) and CD7(Ac), it was eventually possible to derive the hydrodynamic radius to 0.9 ± 0.1 nm from eq 20 given in the Appendix.

An independent attempt was made to evaluate the size of monomeric units from ^{1}H NMR PGSE experiments. In a regime of diffusive motion, the translational self-diffusion coefficient for a sphere is given by the Stokes−Einstein−Debye eq 15 (see Appendix).[27] By introducing the experimental translational self-diffusion coefficients for both units CD7(Am) or CD7(Ac), the hydrodynamic radius of equivalent spherical molecules was 1.0 ± 0.1 nm for CD7(Am) or CD7(Ac), close to the value obtained from relaxation experiments.

The present measurements are in satisfactory agreement with the estimate from the Quanta molecular model of β-CD (external diameter, 1.4 nm; height, about 1.0 nm). Interestingly, the derived thickness of the hydrodynamic solvent shell is 0.2−0.3 nm. This value compares well with the diameter of a solvating water molecule and it is in line with the results obtained for solvation of water-soluble proteins.[28] Moreover it supports the assumption of the stick boundary condition that has been used to derive the molecular radii of CD7(Am) and CD7(Ac).

Both series of experiments have validated the description of the shape of β-cyclodextrin derivatives obtained with the hydrodynamic approach. First, the assumption of isotropic tumbling was satisfactory, in line with their almost spherical shape. Second, the extracted molecular radii were in fair agreement with a β-cyclodextrin core solvated by a hydration shell whose thickness was close to one solvent diameter.

The CD7(Ac):CD7(Am) Associated Species Is a Dimer. First Experimental Evidence. The first approach to determine the shape of the CD7(Ac):CD7(Am) associated species consisted of extracting the hydrodynamic radius of the equivalent spherical object from NMR experiments as already performed for the monomers. For such a purpose, it was first necessary to examine whether the CD7(Ac):CD7(Am) associated species did not dissociate on the relevant time scale of NMR experiments. A crude calculation performed in the Appendix suggested the associated species CD7(Ac):CD7(Am) to be kinetically stable on the time scales associated with all the present series of NMR experiments. This means that the whole complex CD7(Ac):CD7(Am) could be essentially treated as a single species from the point of view of hydrodynamics in the following discussion.

With the same assumptions as for monomeric units, the hydrodynamic radius of the equivalent CD7(Ac):CD7(Am) spherical object from NMR PGSE experiments was 1.4 ± 0.1 nm. If one considers the associated species to result from assembly of monomeric spheres of hydrodynamic radius equal to 1.0 nm, this intermediate value strongly suggested that (i) the associated species was a dimer since any larger aggregate would lead to much lower translational diffusion coefficients[29] and (ii) the assumption of isotropic tumbling for the treatment of the complex data was inappropriate.

Moreover, the determination of the 1:1 stoichiometry made possible attribution of the association constants that were obtained in the previous study[12] to a true dimerization process. Hence, the large values derived from potentiometry do not result from an artifact caused by a dimerization−aggregation process.[30]

Description of the CD7(Ac):CD7(Am) Dimer. In relation to the expected axially symmetrical interaction between monomeric units, three different models have been selected to describe the CD7(Ac):CD7(Am) shape: ellipsoid, cylinder, and dumbbell (Figure 4). Each shape can be characterized by two of the following geometrical parameters: its hydrodynamic length *L*, its hydrodynamic diameter *D*, and its aspect ratio *L*/*D*. In the present case, we considered the diameter *D* to be determined by the cyclodextrin backbone and we fixed its value to 2.0 nm as obtained from NMR experiments on CD7(Am) and CD7(Ac) monomeric units.

The ellipsoidal geometry is not very satisfying from the point of view of the structural description. Indeed it seems rather arbitrary to locate the positions of the interacting cyclodextrins within the ellipsoid. In contrast, the ellipsoidal geometry is the only one for which analytical expressions of translational and rotational diffusion coefficients are available for the whole range of aspect ratios.[31] Furthermore, the spectral densities that have been used to extract the rotational diffusion coefficients from relaxation experiments derived from this geometry (vide infra).[32] The cylindrical and dumbbell shapes seem more appropriate for representing the geometry of the CD7(Ac):CD7(Am) dimer. These shapes can be considered as limiting forms corresponding to a dimer in two extreme regimes of reorientational freedom for each constituting unit: (i) low for the cylinder (in the complex, each monomer has no rotational freedom about an inertial axis that is perpendicular to the symmetry axis of the cylinder) and (ii) large for the dumbbell (each monomer is now freely rotating about its inertial center). In the literature, several expressions linking the different diffusion coefficients to geometrical parameters have been derived from numerical calculations for these geometries.[33]

(27) Equation 15 strictly applies for neutral spheres under the assumption of stick boundary conditions. Due to the low cyclodextrin concentration (2 mM) and the presence of a large concentration of supporting salt (50 mM KCl), this equation is still a good approximation. Indeed under the present conditions, one can neglect both the hydrodynamic coupling between the identically charged cyclodextrins and the Wien effect.

(28) Venable, R. M.; Pastor, R. W. *Biopolymers* **1988**, 1001−1014.

(29) In fact, the analysis is performed on visible NMR signals. It could thus happen that we do not detect large aggregates that lead to very broad peaks. All things being equal, the similarity between the signal/noise ratios for ^{1}H NMR spectra of the CD7(Ac), CD7(Am), and CD7(Ac):CD7(Am) 1:1 mixture suggests that the amount of large aggregates is marginal if any.

(30) Hamelin, B.; Jullien, L. *J. Chem. Soc., Faraday Trans.* **1997**, *93*, 2153-2160.

(31) Perrin, J. *J. Phys. Radium* **1934**, *5*, 497−511. Perrin, J. *J. Phys. Radium* **1936**, *7*, 1−11.

(32) Woessner, D. E. *J. Chem. Phys.* **1962**, *37*, 647−654.

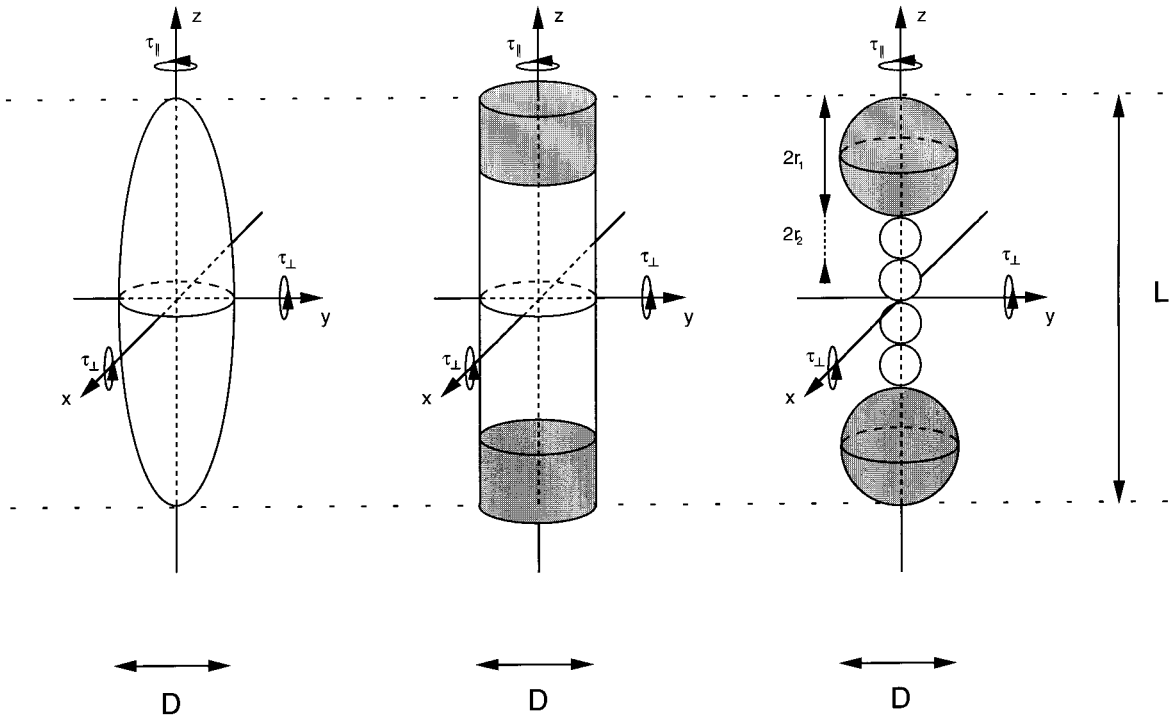

Figure 4. Examined shapes that have been used to describe the CD7(Ac):CD7(Am) dimer. From left to right: ellipsoid, cylinder, and dumbbell. The length *L*, diameter *D*, and at the various correlation times (see text and Appendix) are displayed for each geometry.

Shape Analysis of the CD7(Ac):CD7(Am) Dimer from NMR PGSE Experiments. The translational diffusion coefficients as a function of the aspect ratio *L*/*D* have been simulated for the different envisaged shapes. The corresponding curves then have been used to derive the equivalent hydrodynamical lengths of the dimer from the experimental value of the translational self-diffusion coefficient of CD7(Ac):CD7(Am) (Table 4). Whereas the extracted lengths lie in the same range for the ellipsoid and the dumbbell geometry (5.0 and 4.8 nm), *L* is considerably lower for the cylindrical shape (3.2 nm).

Shape Analysis of the CD7(Ac):CD7(Am) Dimer from NMR Relaxation Experiments. In view of its simplicity, the spectral density function derived from the analysis of the motion of a rigid symmetrically axial ellipsoid has been used for the NOESY simulation.[32,34] Two correlation times describe the ellipsoid rotational motion: $\tau_{||}$ respectively $\tau_\perp$) for the rotation about the symmetry axis (respectively about an inertial axis normal to the symmetry axis). $\tau_{||}$ and $\tau_\perp$ are not independent and both can be calculated as a function of the aspect ratio *L*/*D*.[31] To determine the best fitting values of correlation times, the ^{1}H-NOESY volumes of the CD7(Ac):CD7(Am) dimer have been systematically simulated for the preceding ($\tau_{||}$, $\tau_\perp$) couples by varying the aspect ratio *L*/*D* between 1.5 and 3.2. The derivation of the $\{r_{ij}\}$ set for the CD7(Ac):CD7(Am) dimer required the knowledge of (i) the corresponding set for both constituting units and (ii) the relative orientation of CD7(Am) and CD7(Ac) within the complex. As for the monomers, the

Table 4. Equivalent Hydrodynamical Diameter and Length for the CD7(Ac):CD7(Am) Dimer Under Assumption of Given Shapes As Obtained from PGSE or Relaxation NMR Experiments (See Text and Figure 4)

NMR experiments geometry	PGSE		relaxation	
	D (nm)	*L* (nm)	*D* (nm)	*L* (nm)
ellipsoid	2.0[a]	5.0 ± 0.5[b]	2.0[a]	4.5[c]
cylinder	2.0[a]	3.2 ± 0.5[b]	2.0[a]	3.1[c,d]
dumbbell	2.0[a]	4.8 ± 0.5[b]	2.0[a]	4.0[c,e]

[a] This value is fixed for the whole treatment. [b] The evaluated error results from the experimental incertitude on D_t and temperature during the PGSE NMR experiments. For *L*/*D*, the former was evaluated to be ±0.15 (see Experimental Section) whereas the latter was estimated to be ±0.20. [c] The error on the values extracted from the treatment of relaxation data originates from many sources: (i) incertitude on experimental NOESY volumes that can be neglected with regards to the others; (ii) temperature incertitude (±1 K) [this source leads to an error equal to ±0.015 on *L*/*D*]; (iii) omission of internal motions in the data treatment [from simulations that introduced internal motions, we estimated the incertitude to ±0.25 on *L*/*D*]; (iv) absence of energy minimization on atomic coordinates of CD7(Am) and CD7(Ac). The corresponding error is very difficult to evaluate. Indeed, a possible way to obtain an estimate could be the following. Each V_{Si}^{sim} results from a summation over the seven different configurations adopted by the glucose units contained with the β-cyclodextrin torus. A fictive R_{max} value can be calculated by systematically retaining the individual glucose configuration that yielded the largest deviation from the experimental value. Unfortunately, since extreme glucose configurations cannot simultaneously be adopted due to the cyclization constraint, there is eventually no way to use the difference $R_{max} - R$ to derive even a crude estimate of the error. [d] The error on *L* has two additive sources: (i) the incertitude on the $\tau_{||}$ and $\tau_\perp$ values that have been derived from the relaxation experiments; (ii) $\tau_{||}$ and $\tau_\perp$ do not provide the same aspect ratios. $\tau_{||}$ gives $L/D = 1.45$ whereas $\tau_\perp$ affords $L/D = 1.6$. [e] In contrast to the cylinder case, only $\tau_\perp$ has been used to derive the aspect ratios. Indeed, $\tau_{||}$ is not sensitive to the aspect ratio in the investigated range and $\tau_{||} = 1.75$ ns does not correspond to any simulated value in the investigated *L*/*D* range. The error has been taken identical to the cylinder case.

(33) (a) Garcia De La Torre, J.; Bloomfield, V. A. *Biopolymers* **1977**, *16*, 1747−1763. (b) Garcia De La Torre, J.; Bloomfield, V. A. *Biopolymers* **1977**, *16*, 1765−1778. (c) Garcia De La Torre, J.; Bloomfield, V. A. *Biopolymers* **1977**, 16, 1779−1793. (d) Garcia De La Torre, J.; Bloomfield, V. A. *Q. Rev. Biophys.* **1981**, *14*, I, 81−139. (e) Tirado, M. M.; Garcia De La Torre, J. *J. Chem. Phys.* **1979**, *71(6)*, 2581−2587. (f) Tirado, M. M.; Martinez, C. L.; Garcia De La Torre, J. *J. Chem. Phys.* **1984**, *81*, 2047−2052. (g) Tirado, M. M.; Garcia De La Torre, J. *J. Chem. Phys.* **1980**, *73* 1986−1993. (h) Swanson, E.; Teller, C.; De Haën, D. C. *J. Chem. Phys.* **1978**, *68*, 5097−5102.

(34) Several expressions of spectral density functions are available for the cylinder and dumbbell shapes but their range of applicability is much more limited, especially for low values of the aspect ratio. (a) Cylinder: Lipari, G.; Szabo, A. *J. Chem. Phys.* **1978**, *69*, 1722−1736. (b) Dumbbell: Schurr, J. M.; Babcock, H. P.; Fujimoto, B. S. *J. Magn. Reson.* **1994**, *B105*, 211−224.

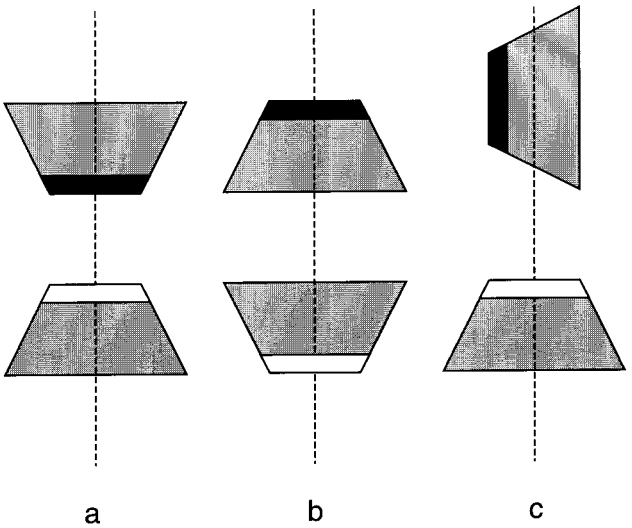

Figure 5. Scheme displaying different relative orientations of interacting monomers in the dimer. Averaged symmetry axis of both monomers aligned: the primary (a) or secondary (b) sides of the oppositely charged cyclodextrins facing each other; perpendicular averaged symmetry axis (c).

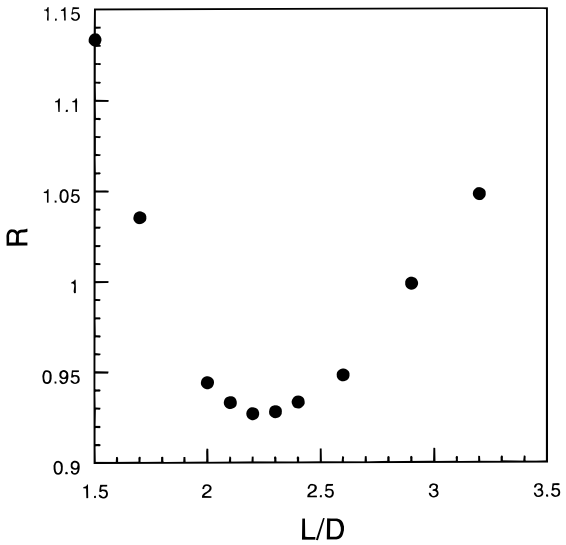

Figure 6. Mean standard deviations between experimental and simulated quantitative NOESY spectra normalized volumes under the assumption of the anisotropic reorientational motion for the CD7(Ac):CD7(Am) dimer. See the Experimental Section and text.

set of Cartesian coordinates of methine protons borne by the cyclodextrin backbone reported for the native β-cyclodextrin has been used to derive the individual $\{r_{ij}\}$.

In a first step, the simulations have been performed for a relative orientation of interacting units in the dimer where both averaged symmetry axes were aligned and where the primary sides of the oppositely charged cyclodextrins were facing each other (Figure 5a). Figure 6 displays the mean standard deviation R between experimental and simulated data as a function of L/D. A minimum is observed for the aspect ratio $L/D = 2.25$ that corresponds to $\tau_{||} = 1.75$ ns and $\tau_{\perp} = 3.7$ ns.

To evaluate the sensitivity of this method for shape determination, different relative orientations of interacting cyclodextrins within the dimer have been generated and the corresponding ^{1}H-NOESY spectra have been simulated for an aspect ratio equal to 2.25. The mean standard deviation between experimental and simulated data for the configuration where both averaged symmetry axes were aligned and where the secondary sides were facing each other (Figure 5b) is equal to the value obtained for the configuration with facing primary faces (Figure 5a). Thus relaxation experiments cannot be used to determine the relative orientations of the cyclodextrin faces. We also simulated the ^{1}H-NOESY spectrum for an extreme configuration with a perpendicular symmetry axis (Figure 5c). The corresponding mean standard deviation was significantly larger than that for the other relative orientations (compare 0.97 to 0.92 with regards to Figure 6). This observation suggested that the contribution from configurations with nearly perpendicular CD relative orientations played a minor role if any in the dimer average description and consequently refuted the dumbbell as a satisfactory description of the dimer geometry.

From the description of molecular units as rigid bodies, it was possible to convert the parallel and perpendicular rotational diffusion coefficients as extracted from the treatment of NMR data into geometric parameters for other shapes than ellipsoidal. From the best preceding fitting values $\tau_{||} = 1.75$ ns and $\tau_{\perp} = 3.7$ ns, the corresponding dimer aspect ratios L/D were determined for the cylinder[24,33f,g] and dumbbell[33d,34b,35] geometries. The results are displayed in Table 4. The values extracted from relaxation experiments satisfactorily compare with those obtained from PGSE NMR experiments. The largest discrepancy was observed for the dumbbell description and probably confirmed the inappropriateness of this model. In contrast, very good agreement was obtained for the cylindrical description, which suggested this shape to be the most suitable representation of the CD7(Ac):CD7(Am) dimer.

Relative Orientation of the Monomeric Units within the CD7(Ac):CD7(Am) Dimer. In the absence of intermolecular NOESY cross-peaks between CD7(Am) and CD7(Ac) in the CD7(Ac):CD7(Am) dimer, the relative orientation of both interacting cyclodextrins within the dimer can only be deduced from the modifications of the different features of CD7(Am) and CD7(Ac) upon association. It has already been emphasized that relaxation NMR experiments or chemical shifts cannot be used to distinguish between the orientations a and b displayed in Figure 5. In fact, a useful piece of information lies in the rotamer analysis that suggested a significant change in the positions of the 6-substituents of CD7(Am) and CD7(Ac) upon dimerization. The contribution of the GT conformation was shown to increase at the expense of the GG conformation in the dimer. The large GG contribution in monomeric units appears in agreement both (i) with the rotamer distribution for native CDs in solution[36] and (ii) with the repulsive interaction between mobile charged headgroups that forces them to move apart from the molecule symmetry axis.[37] In striking contrast, the drop of the contribution of the GG conformation in the dimer points to (i) the attractive interaction between oppositely charged groups and (ii) a decrease in the repulsion between intramolecular charges resulting from CD7(Am):CD7(Ac) dimerization. If one additionally considers that the Gibbs free energy of association between oppositely charged bodies is a decreasing function of the distance,[38] the observation that the outwardly pointing arms bearing the charged groups go from an approximately perpendicular to a parallel average orientation with regards to the cyclodextrin symmetry axis strongly suggests that the configuration displayed in Figure 5a satisfactorily represents the dimer CD7(Am):CD7(Ac).

(35) Small, E. W.; Anderson, S. R. *Biochemistry* **1988**, *27*, 419−428.
(36) Wood, D. J.; Hruska, F. E.; Saenger, W. *J. Am. Chem. Soc.* **1977**, *99*, 1735−1740. Lindner, K.; Saenger, W. *Carbohydr. Res.* **1982**, *99*, 103−115.
(37) Compare the average distance between adjacent 6-glucose positions (about 1 nm) with the inverse Debye length at 50 mM KCl (about 1.5 nm).
(38) Parsegian, V. A.; Gingell, D. *Biophys. J.* **1972**, *12*, 1192−1204.

Once the aspect ratio and the relative orientation of monomeric units were determined, it was possible to extract the distance between the interacting cyclodextrins for the cylindrical geometry. Upon considering that cylinder extremities directly corresponded to the cyclodextrin secondary faces covered by a strongly adhering hydrodynamic layer whose thickness was equal to one solvent diameter $\varnothing_s$, a crude estimate of the distance z_{eq}^{cyl} between both units was obtained from the formula:

$$z_{eq}^{cyl} = L - (h_+ + h_-) - 2\phi_s \qquad (2)$$

where h_+ and h_- represented the respective heights of the positively and negatively charged units estimated from Quanta molecular models. Upon considering that $h_+ = 0.8$ nm and $h_- = 1.2$ nm and additionally taking $\phi_s = 0.25$ nm as suggested by data analysis for CD7(Am) and CD7(Ac), $z_{eq}^{cyl} = 0.6 \pm 0.5$ nm was obtained. This estimate is in agreement with the absence of cross-peak between any couple of protons belonging to the CD7(Am) and CD7(Ac) monomeric units within the CD7-(Am):CD7(Ac) dimer that suggested $z_{eq}^{cyl} \geq 0.4$ nm. This finally yields 0.4 nm $\leq z_{eq}^{cyl} \leq$ 1.1 nm with a maximum probability at 0.6 nm. Such a value can be understood if one analyzes the electrostatic interaction in water.[39] At long interionic separations, the continuum model for water description applies and the attractive interaction is expected to exhibit a screened hyperbolic dependence on distance. At short interionic separations, the loss of the hydration energy for oppositely charged ions is greater than the gain in Coulomb energy. The interionic potential of mean force between oppositely charged bodies is thus expected to display a shallow minimum in the range of 2−3 diameters of water molecules. This result does not necessarily mean that the observed equilibrium distance z_{eq} corresponds to the absolute minimum of energy as a function of the distance between interacting molecules. One cannot thus exclude that a deeper minimum exists at a much smaller distance but the energy barrier between these two minima could be too large to be crossed under the present experimental conditions. Such a two-step docking process already has been suggested to occur in biological systems.[40]

Conclusion

The present study demonstrates that a molecular capsule based on charge−charge interaction can be built in aqueous solution. The association between oppositely highly charged β-cyclodextrin derivatives in water is a dimerization that brings charged faces close to each other. The complexation of suitable subtrates and the examination of their properties within the self-assembled capsule are under study.

The present study also validates the use of NMR dynamic methods to investigate self-assembled arrays in solution. Despite reducing molecules to smooth rigid bodies, this approach provides useful information about the average structure (shape and volume) of associated species.

Eventually, in addition to its relevance for the field of supramolecular chemistry, this investigation provides an estimate of the equilibrium distance between oppositely charged bodies in diluted aqueous solution. The extracted 0.6 nm value has been shown to satisfactorily lie in the range predicted by several theories related to ionic interactions in water.

Experimental Section

Preparation of NMR Samples. In a first step, the aqueous solubility of the CD7(Am):CD7(Ac) 1:1 associated species has been shown to be equal to 1.4 mM at 20 °C from ^{1}H NMR signal integration with ethanol as the internal standard of known concentration. Aqueous solutions of CD7(Am) (2 mM), CD7(Ac) (2 mM) and CD7(Am):CD7-(Ac) 1:1 (1 mM) in KCl (50 mM) then have been titrated by NaOH or HCl (0.1 M) until the appropriate pH has been reached with stirring. The corresponding solutions have been lyophilized three times from D_2O 99.8% and then solubilized in the original volume of D_2O 99.9%.[41] Five millimeter NMR tubes have been filled with 0.5 mL of solution, submitted to freeze−thaw cycles under argon and high vacuum, and finally sealed under vacuum.

NMR Spectroscopy. The temperature has been classically calibrated by measuring the separation between the two lines from a sample of glycol in DMSO-d_6. ^{1}H NMR chemical shift are given in ppm by using DSS (3-trimethysilylpropanesulfonic sodium salt: Merck; $\delta(CH_3) = 0.015$ ppm in D_2O) as an internal reference. ^{1}H NMR correlation spectra (phase-sensitive COSY-DQF and NOESY) were acquired at 400.13 MHz on either an AM or a DRX Bruker spectrometer with standard pulse sequences at 294 ± 1 K. Rotamer populations have been extracted from experimental $^3J_{5,6i}^{exp}$ (i = a or b) coupling constants by considering the three staggered conformers: GG (O5−C5−C6−O6 dihedral, 60°; C4−C5−C6−O6 dihedral, 60°), GT (O5−C5−C6−O6 dihedral, 60°; C4−C5−C6−O6 dihedral, 180°), and TG (O5−C5−C6−O6 dihedral, 180°; C4−C5−C6−O6 dihedral, 60°), whose corresponding theoretical coupling constants $^3J_{5,6i}^{th}$ are available in the literature.[42] The respective populations p_{GG}, p_{GT}, and p_{TG} are obtained by solving the system of linear equations:

$$^3J_{5,6i}^{exp} = p_{GG}\,{}^3J_{5,6i}^{GG,th} + p_{TG}\,{}^3J_{5,6i}^{TG,th} + p_{GT}\,{}^3J_{5,6i}^{GT,th} \qquad i = a \text{ or } b \quad (3)$$

$$1 = p_{GG} + p_{TG} + p_{GT} \qquad (4)$$

Two sets of NOESY spectra were recorded with mixing times τ_m of 0 and 400 ms, for all samples: CD7(Am), CD7(Ac), and CD7(Am):CD7-(Ac) 1:1 mixture. The recycle time was set to 5 times the longest T_1 (11 s) to obtain a symmetrical normalized NOESY volume matrix. The normalization procedure is stepwise.[19] First, the diagonal and cross-peaks intensities are evaluated from the summed $\omega 1$ subspectra contributing to a specific signal. The raw NOESY volumes for τ_m = 400 ms are then divided by the average diagonal volume for one spin for $\tau_m = 0$ s. These corrected NOESY volumes are subsequently divided by the number of spins in the considered signals to yield the values given in Table 3. Integration of noise gave roughly ±0.005 units of normalized intensity with respect to the diagonal volume ($\tau_m = 0$ s) for typical peak widths. PGSE experiments have been performed in ^{1}H NMR at 600 MHz on a Bruker DRX spectrometer at 294 ± 1 K. The stimulated spin−echo sequence[43] has been used to minimize phase distortion present in the simple spin−echo pulse scheme as well as loss of signal due to transverse relaxation. We chose to vary the gradient duration from 0.4 to 2.6 ms by steps of 0.2 ms, while keeping its strength fixed at 21.5 G/cm. The intergradient delay Delta was set to 103 ms, during which magnetization spent only 6 ms in the transverse plan. The translational self-diffusion coefficients have been extracted, according to the Stejskal-Tanner equation,[44] after recording the peak intensities as a function of the gradient length on 10−12 points. Separate measures of the H1 peaks and the nonanomeric peaks have allowed an estimation of the uncertainty made on the determination of these coefficients.

Simulation of NOESY Spectra. In view of the signal overlap between the different spins, simulations have been performed on seven ensembles corresponding to the sum of individual signals: S1 = [H1-

(39) Rashin, A. A. *J. Phys. Chem.* **1989**, *93*, 4664−4669.
(40) Zacharias, M.; Luty, B. A.; Davis, M. E.; McCammon, J. A. *Biophys. J.* **1992**, *63*, 1280−1285.
(41) The solvent isotopic effect on pH scale resulting from changing from H_2O to D_2O is expected to slightly shift acidobasic equilibria (pD = pH(meter reading) + 0.4 according to: Wütrich, K. *NMR in Biological Research: Peptides and Proteins*; North-Holland Publishing Company: Amsterdam, 1976). Nevertheless, the present hydrodynamic study does not deal with protonation states but with association.
(42) Haasnoot, C. A. G. *Tetrahedron* **1980**, *36*, 2783−2792.
(43) Tanner, J. E. *J. Chem. Phys.* **1970**, *52*, 2523−2526.
(44) Stejskal, E. O.; Tanner, J. E. *J. Chem. Phys.* **1965**, *42*, 288−292.

(Ac) + H1(Am)]; S2 = [H5(Am)]; S3 = [H3(Ac) + H3(Am) + H5-(Ac)]; S4 = [H2(Ac) + H2(Am) + H4(Ac) + H4(Am)]; S5 = [H6a(Am) + SCH_2(a and b)(Ac)]; S6 = [H6a(Ac) + H6b(Am)]; S7 = [H6b(Ac)]. The intensity threshold of the NOESY signal has been taken equal to 0.03 for data analysis. The theoretical NOESY volumes were back-calculated from the distance matrix of the CD7(Am) and CD7(Ac) structures with in-house software.[45] The Cartesian coordinates of the cristallographic β-cyclodextrin−ethanol complex structure[46] were transformed into CD7(Am) and CD7(Ac) structures with the Quanta 4.0 commercial package (MSI Inc). The two interacting units were positioned as displayed in Figure 5 with the plane containing anomeric oxygen atoms and the symmetry axis as reference plane and axis respectively for defining cyclodextrin orientation. The relaxation constants R_{ii} and R_{ij} (eqs 5 and 6) have been calculated from the transition probabilities by using the full-matrix approach[47] as follows:

$$R_{ii} = \sum_j (W_0^{ij} + 2W_1^{ij} + W_2^{ij}) \tag{5}$$

$$R_{ij} = (W_2^{ij} - W_0^{ij}) \tag{6}$$

where W_0, W_1, and W_2 are the zero-, single-, and double-quantum transition probabilities. No other source of relaxation was considered since it has been shown that the dipolar interaction is the dominating relaxation source for sugars in ^{1}H NMR.[17] The transition probabilities are in turn written as:

$$W_0^{ij} = J(\omega_i - \omega_j) \tag{7}$$

$$W_1^{ij} = 1.5J(\omega_i) \tag{8}$$

$$W_2^{ij} = 6J(\omega_i + \omega_j) \tag{9}$$

where $J(\omega)$ is the spectral density function describing the motion of the dipolar coupled nuclei. Two cases were considered for describing the molecular dynamics of the diverse species involved in the present study: (1) a rigid body undergoing isotropic overall tumbling (for the monomers CD7(Am) and CD7(Ac)) and (2) a rigid body undergoing anisotropic axially symmetrical overall tumbling (for the CD7(Am):CD7(Ac) dimer). The corresponding spectral densities are given in the following equations:

$$\text{Case 1:} \quad J_{iso} = q_{ij}\frac{\tau_c}{(1+\omega^2\tau_c^2)} \tag{10}$$

$$\text{Case 2:} \quad J_{aniso} = q_{ij}\left[0.25\frac{(3\cos^2\theta - 1)^2\tau_a}{(1+\omega^2\tau_a^2)}\right] + \left[\frac{3\sin^2\theta\cos^2\theta\tau_b}{(1+\omega^2\tau_b^2)}\right] + \left[0.75\frac{\sin^4\theta\tau_c}{(1+\omega^2\tau_c^2)}\right] \tag{11}$$

where $q_{ij} = 0.1\gamma_H^4\hbar^2 r_{ij}^{-6}$, $\tau_a = \tau_\perp$, $1/\tau_b = 5/(6\tau_\perp) + 1/(6\tau_{||})$, $1/\tau_c = 1/(3\tau_\perp) + 2/(3\tau_{||})$, and θ is the angle between the relaxation vector and the symmetry axis.[32]

The mean standard deviation R between simulated and experimental data has been calculated according to the formula:

$$R = \sqrt{\sum_{Si}\left(\frac{V_{Si}^{sim} - V_{Si}^{exp}}{V_{Si}^{exp}}\right)^2} \tag{12}$$

where Si, V_{Si}^{sim} and V_{Si}^{exp}, respectively, designate the ensemble of spins H1 to H5, the corresponding simulated and experimental normalized diagonal and cross NOESY volumes under the conditions $V_{Si}^{sim} \geq 0.03$ and $V_{Si}^{exp} \geq 0.03$.

η_{294K}(KCl 50 mM) = 0.98 cP = 0.98 10^{-3} Pa·s[48] has been used to simulate hydrodynamic data according to the formula that are given in the Appendix.

Acknowledgment. L.J. is very much indebted to Drs. L. Belloni, R. Lavery, G. Orädd, M. Schurr, and D. C. Teller for providing helpful discussions related to this work. Drs. H. Driguez and L. De Robertis are gratefully acknowledged for their essential participation to the synthesis of CD7(Ac).

Appendix

Kinetic Stability of the CD7(Ac):CD7(Am) Complex. Data interpretation for the different NMR measurements requires the determination of the lifetime of the associated species (τ_{ass}) in relation to the significant time scales relevant for both NMR experiments: about 1 ns for relaxation measurements and 1 ms for the determination of translational self-diffusion coefficients. An estimate of τ_{ass} can be calculated by assuming (i) the association rate is controlled by diffusion of interacting cyclodextrins toward each other and (ii) any collision between oppositely charged species yields association.[49] Then a crude order of magnitude can be obtained by applying the following expression giving the number G of collisions per unit of time between interacting spherical colloids:[50]

$$G = 8\pi D_t n_0 / \int_{R_1+R_2}^{+\infty} \frac{1}{r^2} e^{\varphi_{12}/kT}\, dr \tag{13}$$

with:

$$\varphi_{12} = \frac{z_1 z_2 e^{-\kappa r}}{4\pi\epsilon_0\epsilon_r(1+\kappa R_1)(1+\kappa R_2)r} \tag{14}$$

where D_t is the translational self-diffusion coefficient (see eq 15 in Appendix), R_1 and R_2 are the radii, n_0 is the concentration of the interacting colloids, η is the solvent viscosity, and κ^{-1} is the Debye−Hückel reciprocal length of the solution. Under the assumption that the cyclodextrins are identical but bearing opposite charges and if taking $\eta = 10^{-3}$ Pa·s, $R_1 = R_2 = R =$ 1 nm, $n_0 = 2$ mM $= 1.2 \times 10^{21}$ molecules/L, $|z_1| = |z_2| = 7|e|$ (e is the elementary charge), $\kappa^{-1} = 2$ nm, the numerical integration of the previous expression provides:

$$G \approx 2 \times 10^4 \text{ collisions/s}$$

It is then possible to estimate the lifetime τ_{unit} of the free interacting units:

$$\tau_{unit} \approx 1/G = 40\ \mu\text{s}$$

and thus

(45) Bouchemal-Chibani, N.; Braccini, I.; Derouet, C.; Hervé du Penhoat, C.; Michon, V. *Int. J. Biol. Macromol.* **1995**, *17*, 177−182.

(46) Steiner, T.; Mason, S. A.; Saenger, W. *J. Am. Chem. Soc.* **1991**, *113*, 5676−5687.

(47) Olejniczack, E. T.; Gampe, R. T., Jr.; Fesik, S. W. *J. Magn. Reson.* **1986**, *67*, 28−41.

(48) *Handbook of Chemistry and Physics*, 61st ed.; CRC Press Inc.: Boca Raton, 1980−1981.

(49) In the present system, the duration of an encounter between the interacting oppositely charged units is much larger than the rotation time required to orient into the most stable associated species. The capture efficiency can thus be reasonably assumed to remain close to one to derive a crude estimate. For references on electrostatics in the Brownian dynamics of association in complex systems, see for instance: Northrup, S. H.; Boles, J. O.; Reynolds, J. C. L. *J. Phys. Chem.* **1987**, *91*, 5991−5998 and references therein.

(50) Verwey, E. J. W.; Overbeek, J. Th. G. *Theory of the Stability of Lyophobic Colloids*; Elsevier: New York, 1948.

$$\tau_{ass} \approx \langle K \rangle \tau_{unit} \approx 10^4 - 10^5 \text{ s}$$

with $\langle K \rangle = 10^{10}$.[12] τ_{ass} exceeding by far 10^{-3} s, this crude calculation suggests the associated species CD7(Ac):CD7(Am) to be kinetically stable at the time scales associated with all the present series of NMR experiments.[51]

Expressions of Translational Self-Diffusion Coefficients and Correlation Times (Stick Boundary Conditions). (a) Translational Self-Diffusion Coefficients. (i) Sphere[13]

$$D_t^{sphere} = \frac{kT}{6\pi\eta R} \tag{15}$$

where k is the Boltzmann constant, T the absolute temperature, η the medium viscosity, and R the sphere radius.

(ii) Prolate Ellipsoid.[31]

$$D_t = \frac{\rho^{2/3} D_0}{\sqrt{1-\rho^2}} \ln\left(\frac{1+\sqrt{1-\rho^2}}{\rho}\right) \tag{16}$$

where a and b are the z and x semi-axis of the ellipsoid ($a > b$), $\rho = D/L$, and D_0 designates the self-diffusion coefficient of the equivalent sphere of the same volume:

$$D_0 = \frac{kT}{6\pi\eta a}\rho^{-2/3} \tag{17}$$

(iii) Right Circular Cylinder. A semiempirical formula is available in the range $2 \le p = L/D \le 30$.[33f]

$$D_t = \frac{kT(\ln p + \nu)}{3\pi\eta L}$$

with

$$\nu = 0.312 + 0.565/p - 0.100/p^2 \tag{18}$$

Another work, in fair agreement with experimental results, reports translational self-diffusion coefficients for different values of p.[33h] In view of our experimental errors, the agreement between experimental and semiempirical results[33h] and between data contained in both refs 33f and 33h pushed us to extrapolate eqs 20, 21, and 22 up to $p = 1$.

(iv) Dumbbell. Two large spheres (radius r_1; $D = 2r_1$) are connected by a rod of smaller spheres at contact (radius r_2). The following semiempirical expression has been used to derive D_t:[33a]

$$D_t = \frac{kT}{6\pi\eta r_i}\left[\frac{4}{3} + \sum_{i=1}^{3}\sum_{j=1}^{3} b_{ij}\left(\frac{L=4r_1}{r_1}\right)^i\left(\frac{r_1}{r_2}\right)^{j-1}\right]^{-1} \tag{19}$$

Another set of semiempirical data corresponding to $r_2 = 0$ has also been used for comparison.[33h]

(b) Correlation Times. (i) Sphere. With the same notations as in the last paragraph, the correlation time τ_c around any axis containing the sphere center that is measured by NMR relaxation experiments is

$$\tau_c = \frac{4\pi\eta R^3}{3kT} \tag{20}$$

(51) In particular for the treatment of PGSE ^{1}H NMR data. See: Kärger, J. *Ann. Phys.* **1969**, *24*, 1−4. Kärger, J. *Ann. Phys.* **1971**, *27*, 107−109.

(ii) Prolate Ellipsoid. With the same notations as before:[31]

$$1/(6\tau_\perp) = \frac{3kT[(2a^2-b^2)S - 2a]}{32\pi\eta(a^4-b^4)} \tag{21}$$

$$1/(6\tau_{||}) = \frac{3kT(2a - b^2 S)}{32\pi\eta(a^2-b^2)b^2} \tag{22}$$

with

$$S = \frac{2}{\sqrt{a^2-b^2}} \ln\left(\frac{a+\sqrt{a^2-b^2}}{b}\right) \tag{23}$$

(iii) Right Circular Cylinder. Semiempirical formula are obtained for $\tau_\perp$ and $\tau_{||}$ in the range $2 \le p = L/D \le 30$. With the same notations as above:[24,33f,g]

$$1/(6\tau_\perp) = \frac{3kT(\ln p + \delta_{perp})}{\pi\eta L^3}$$

with

$$\delta_{perp} = -0.662 + 0.917/p - 0.050/p^2 \tag{24}$$

$$1/(6\tau_{||}) = \frac{4kT}{A\pi\eta L D^2(1+\delta_{paral})}$$

with

$$A = 3.841 \text{ and } \delta_{paral} = (1.119 \times 10^{-4}) + 0.6884/p - 0.2019/p^2 \tag{25}$$

As previously justified, we extrapolated eqs 24 and 25 up to $p = 1$. In fact, the authors of ref 24 mention themselves that these equations would probably apply below $p = 2$ fairly well.

(iv) Dumbbell. With the same notations as in the last paragraph, the following semiempirical expression has been used to derive $\tau_\perp$:[33d,34b,35]

$$1/(6\tau_\perp) = \frac{0.2675kT}{8\pi\eta {r_1}^3} \exp\left[\sum_{i=1}^{3}\sum_{j=1}^{3} c_{ij}\left(\frac{L-4r_1}{r_1}\right)^i\left(\frac{r_2}{r_1}\right)^{j-1}\right] \tag{26}$$

$\tau_{||}$ is obtained by summing the individual rotational diffusion coefficients of the constituting spheres of the dumbbell.[35]

$$1/(6\tau_{||}) = \sum_{\text{spheres}} \frac{kT}{8\pi\eta r_{sphere}^3} = \frac{kT}{8\pi\eta\left(2{r_1}^3 + \frac{(L-4r_1)}{2r_2}{r_2}^3\right)} \tag{27}$$

Supporting Information Available: Figures showing the comparison of experimental and simulated ^{1}H NMR chemical shifts of CD7(Am) as a function of pH for H1 and H6a signals, simulation of translational self-diffusion coefficients as a function of the aspect ratio L/D for different geometries, dependence of the correlation times $\tau_{||}$ and $\tau_\perp$ as a function of the aspect ratio L/D for the symmetrically axial ellipsoidal shape, and simulation of the correlation times $\tau_{||}$ and $\tau_\perp$ as a function of the aspect ratio L/D for different geometries (5 pages; print/PDF). See any current masthead page for ordering information and Web access instructions.

JA980046G